Supplementary Information

Multiple Active Site Additive-Mediated Suppression of Sn^{2+} Oxidation and Regulation Crystallization for High-Performance Sn-Pb Mixed Perovskite Solar Cells

Cheng Li,[a] Mingzhe Zhu,[a] Haokun Jiang,[a] Shuming Zhang,[a] Jiahui Cheng,[a] Huijie Cao,[a] Tao Wang,*[a] and Zhongmin Zhou*[a]

Materials and Solvents

All chemicals and reagents are used directly upon receipt without further processing. Tin (II) iodide (SnI_2, 99.999%) was purchased from Sigma Aldrich. Athocuproline (BCP,>99%) and PEDOT: PSS (CLEVIOS P VP AI 4083 from Heraeus) were purchased from Xi'an Polymer Light Technology Co., Ltd. (FAI), while methylammonium iodide (MAI, ≥ 99.5%) and lead (II) iodide (PbI_2) were purchased from Aladdin Ltd. Tin (II) fluoride (SnF_2, 99%), cesium iodide (CsI,>99.0%), and N-Hydroxythiophene-2-Carboximidamide (NHC, ≥ 98%) were purchased from Aladdin. Dimethyl sulfoxide (DMSO, 99.9%, Acros), N, N-dimethylformamide (DMF, 99.8%, Acros), isopropanol (IPA, 99.5%, Acros), ether (Acros), chlorobenzene (CB, 99.8%, Acros), and methanol (Acros) are from Beijing Inokai Chemical Technology Co., Ltd.

Precursor Solution Preparation

$FA_{0.7}MA_{0.2}Cs_{0.1}Pb_{0.5}Sn_{0.5}I_3$ precursor solution with a molar concentration of 1.8 M. Specific preparation process: Dissolve FAI (1.26 mmol), MAI (0.36 mmol), PbI_2 (0.9 mmol), CsI (0.18 mmol), SnI_2 (0.9 mmol), and SnF_2 (0.045 mmol) in a DMF: DMSO mixed solvent (v: v=3:1) in a nitrogen glove box. Finally, 1g/mL NHC was added to the perovskite precursor. Finally, stir the mixed solution at room temperature for 2.5 hours ◦

Device Fabrication for Sn-Pb PSCs

Clean and treat ITO glass substrate with O_3 plasma for 500 s. After ultrasonic treatment of PEDOT: PSS dispersion for 20 min, the obtained dispersion was rotated onto the treated ITO at a speed of 4000 rpm for 30 s and annealed at 150°C for 20 min. Then quickly transfer the annealed ITO/HTL to a nitrogen glove box for manufacturing other functional layers. Before use, filter the perovskite precursor solution through a 0.22 μm PTFE filter, then rotate the perovskite precursor solution onto ITO/ETL at a speed of 1000 rpm for 10 s, and then rotate it at a speed of 4500 rpm for 60 s. Inject CB anti solvent 20 s before the end of the spin coating. Annealing the obtained film at 100 °C for 10 min to obtain a perovskite layer. After waiting for the film to cool to room temperature, rotate the PCBM onto the film at a speed of 1200 rpm for 25 s. Subsequently, BCP was dynamically rotated on the PCBM at a speed of 5500 rpm for 25 s. Finally, evaporate 70 nm Ag as an electrode on the top layer.

Devices Characterization:

Fourier transform infrared (FTIR) spectroscopy was characterized using Nicolet iS50 (Thermo Scientific). FTIR test samples were prepared by spin-coating pure NHC and NHC mixtures with different components of perovskites before and after substrate heating. The sample was scraped off the substrate and laminate and mixed with KBR for tableting (sample: KBr = 1:100). XPS spectroscopy of perovskite films on ITO used the Thermo Fisher ESCALAB 250 Practice. Curve fitting was performed using Thermo Avantage software. XRD patterns were measured with Ultima IV of Cu Kα radiation (1.5406 Å). UV-vis absorbance is measured by UV/vis spectrometer. N_2 Stability: The unit was stored in a nitrogen glove box and each test was performed in an air atmosphere with low relative humidity. (Humidity Stability Test) Place the unpacked device in a dark environment protected from 40 ± 5% RH. The temperature is about 25 °C. (Thermal Stability Test) Place the unpacked device on a light-shielded heating plate at 70 °C. The light source consists of a set of white LEDs powered by constant current (SLS-LED-80, Qingdao Solar Science Instrument Technology Co, Ltd.). Sunlight intensity is calibrated by a calibrated Si reference cell. During the aging process, the device was masked and placed in an environment purged with a continuous N_2 stream. *J–V* curves with reverse voltage sweeps were performed every 8 h throughout the running test.

Characterizations

UV-vis

UV-vis spectra of perovskite film on ITO were characterized on UV-2600 spectrophotometer (Agilent Technologies Inc. Cary 5000 spectrophotometer), where ITO glass was the blank control.

J–*V* characteristics

The *J*–*V* characteristics at the maximum power output bias of the device were recorded under AM1.5G illumination of 100 mW cm^{-2} using a solar simulator (PV Measurements eristics (voltage sweep rate of 10 mV/30 ms) and the steady-state photocurrent). Under ambient conditions, the *J*–*V* curves of all devices are measured by masking devices with a metal mask with a hole area of 0.09 cm^2. The standard Si solar cell was used to correct the light intensity of the solar simulator (SLSLED-6060A, Qingdao Solar Scientific Instrument High-tech Co., Ltd)

EQE

The EQE spectra were measured by the QE systems (PV Measurement Inc). with the monochromatic light intensity calibrated by a Si photodiode (Newport, 818-UV).

SEM

The morphology of perovskite films was characterized using SEM (JEOL JSMD7800F Prime)

XRD

The XRD patterns were measured by Ultima IV of Rigaku with Cu Kα radiation (1.5406 Å).

NMR

NMR spectra were recorded on a 400 MHz Bruker AVANCE III 600 NMR spectrometer. The samples were dissolved in DMSO-d_6.

Device stability

Operational stability test was performed using the stability setting (LC Auto-Test 24, Shenzhen Lancheng Technology Co., Ltd.). During the test, all units were unencapsulated and tested under continuous illumination and MPP tracking. The light source consists of a set of white LEDs powered by constant current (SLS-LED-80, Qingdao Solar Science Instrument Technology Co., Ltd.). Calibrate the intensity of sunlight using a calibrated Si reference cell. Thermal stability test: Store the unpackaged device on a thermostatic heating plate at 70 °C for protection from light. Storage Stability Test: Place the unencapsulated battery in air at RH < 25% at a temperature of approximately 25 °C. Storage stability test: The unencapsulated battery is placed in RH < 25% air at an ambient temperature of about 25 °C. Temperature-dependent conductivity test: Conductivity is obtained by measuring current and voltage at different temperatures (-80 to 50 °C), and then the activation energy of ion mobility is calculated from the linear fit data.

Supplementary Note2: Energy loss analysis[1]

The transmission loss (E_{trans}), thermalization energy ($E_{thermal}$), non-absorbing light absorbing (E_{abs}), internal quantum efficiency (E_{IQE}), V_{oc} (E_{Voc}), *FF* (E_{FF}) and total converted energy (E_{conv}) were calculated by the following formulas:

The transmission loss was calculated by：

$$E_{trans} = \int_0^{E_g} \emptyset(hv)\,dhv \#\mathrm{S1}$$

where E_g represents the bandgap of the solar cell system, $\emptyset(hv)$ stands for the solar energy spectrum, and hv is the photon energy.

The insufficient light absorbing loss can be calculated by:

$$E_{abs} = \int_{E_g}^{4.43} [1 - EQE(100\%\ IQE, hv)]\emptyset(hv)dhv \#S2$$

Thermalization energy loss can be calculated by:

$$E_{therm} = \int_{E_g}^{4.43} \left(1 - \frac{E_g}{hv}\right) dhv \#S3$$

Combining E_{abs} and E_{IQE}

$$E_{FF} = (1 - FF)\left[\int_{E_g}^{4.43} \emptyset(hv)dhv - E_{trans} - E_{abs} - E_{therm} - E_{Voc} - E_{IQE}\right] \#S4$$

V_{OC} loss can be calculated by

$$E_{Voc} = \int_{E_g}^{4.43} \frac{E_g - V_{OC}}{hv} EQE(hv)\emptyset(hv)dhv \#S5$$

IQE loss can be calculated by

$$E_{IQE} = \int_{E_g}^{4.43} [1 - IQE(100\%\ EQE, hv)]\emptyset(hv)dhv \#S6$$

FF loss can be calculated by

$$E_{FF} = (1 - FF)\left[\int_{E_g}^{4.43} \emptyset(hv)dhv - E_{trans} - E_{abs} - E_{therm} - E_{Voc} - E_{IQE}\right] \#S7$$

The converted energy can be calculated by:

$$E_{conv} = \int_{E_g}^{4.43} \emptyset(hv)dhv - E_{trans} - E_{abs} - E_{therm} - E_{Voc} - E_{IQE} - E_{FF} \#S8$$

Supplementary Note 2: The space charge limited current (SCLC) method

The N_t can be calculated using the following equation:

$$N_t = \frac{2\varepsilon\varepsilon_0 V_{TEL}}{qL^2} \#S9$$

where ε and ε_0 are relative permittivity and vacuum permittivity, respectively. L stands for the thickness of perovskite film and V_{TFL} represents the onset voltage of the trap-filled limit region.

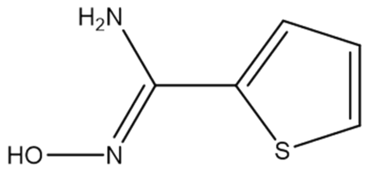

Figure S1. The molecular formula of NHC.

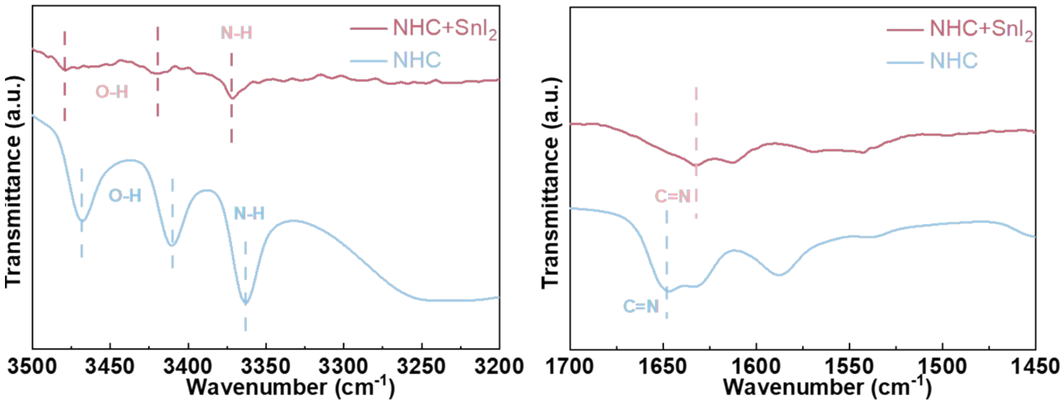

Figure S2. Enlarged FTIR spectra of the NHC and NHC-SnI_2 powders.

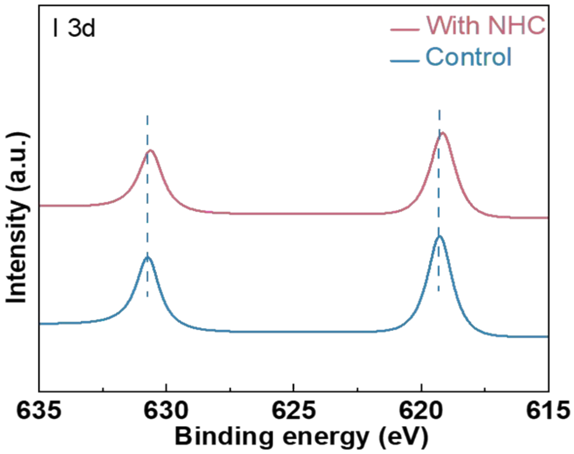

Figure S3. XPS spectra for I 3d orbit of the perovskite films.

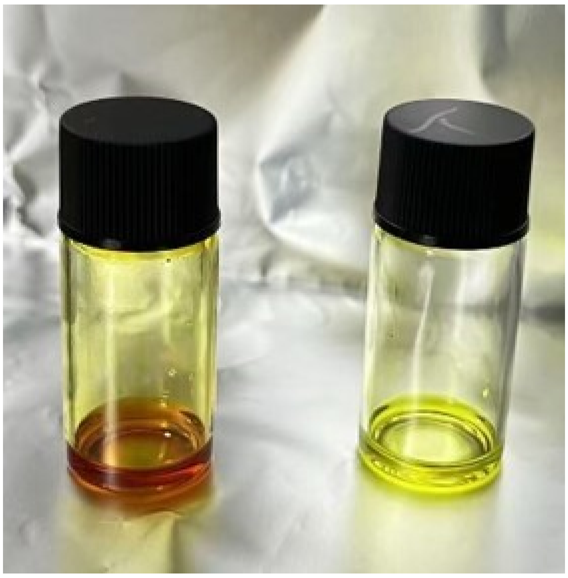

Figure S4. Color change of perovskite precursor solution with or without NHC.

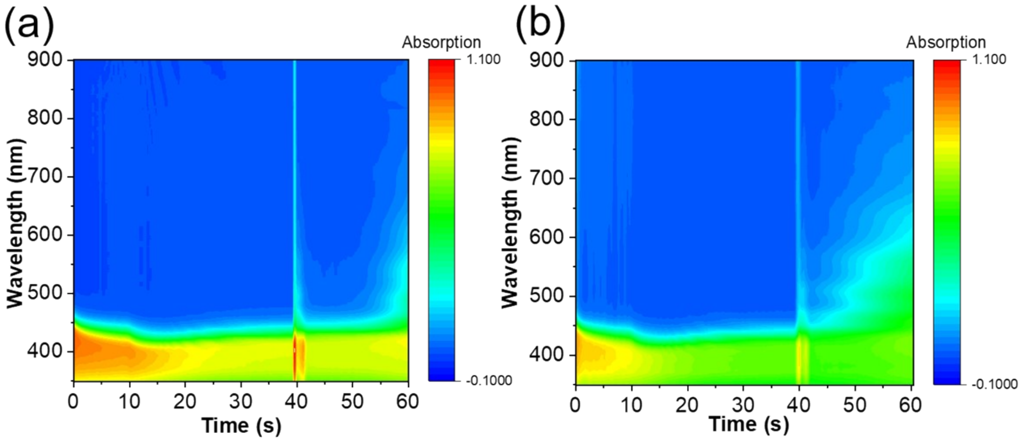

Figure S5. The in situ UV-vis absorption spectra of the perovskite film treated without (a) and with (b) NHC during the spinning process.

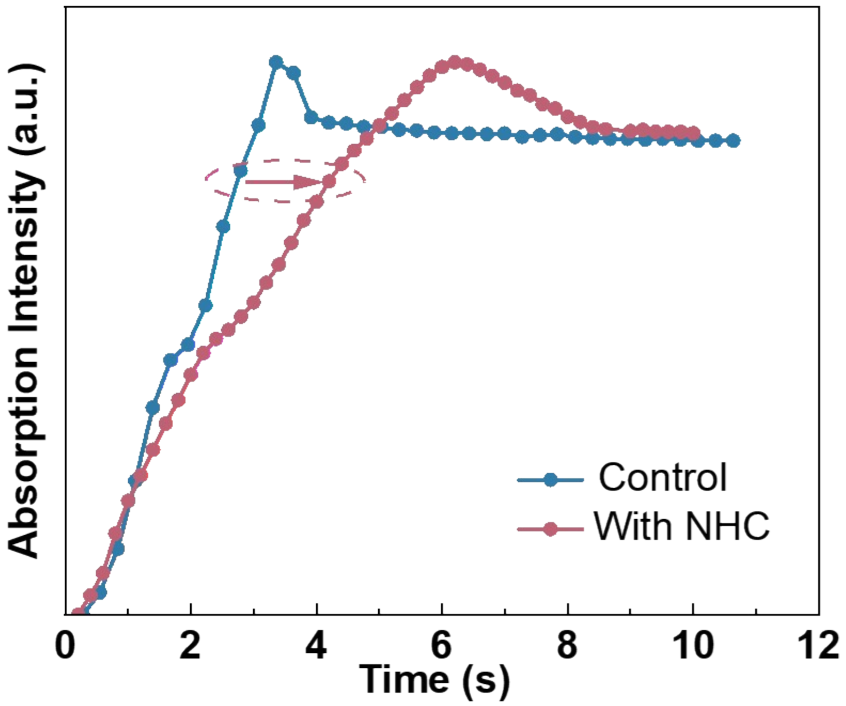

Figure S6. Dynamical evolution of absorption intensity traced at a wavelength of 900 nm for the control and NHC-treated perovskite films during thermal annealing.

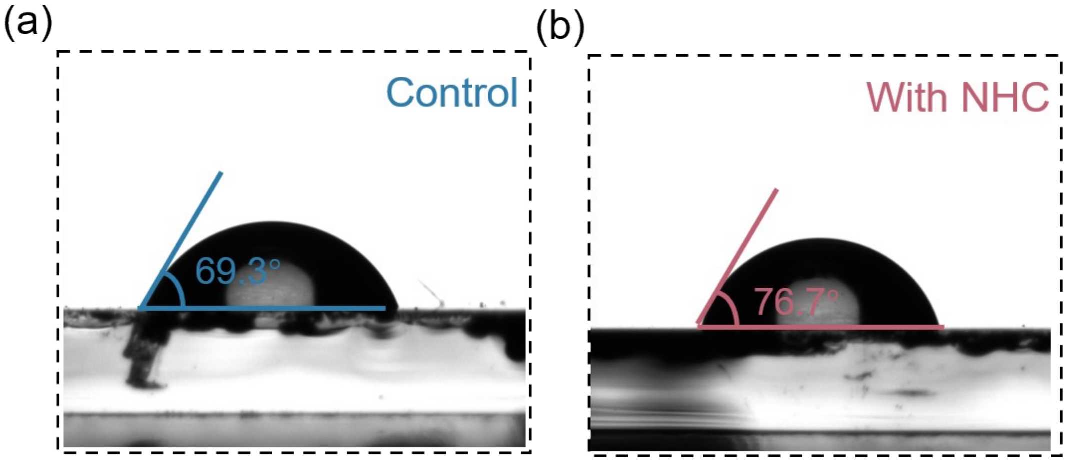

Figure S7. Water contact angle on the (a) control and (b)NHC-treated perovskite films.

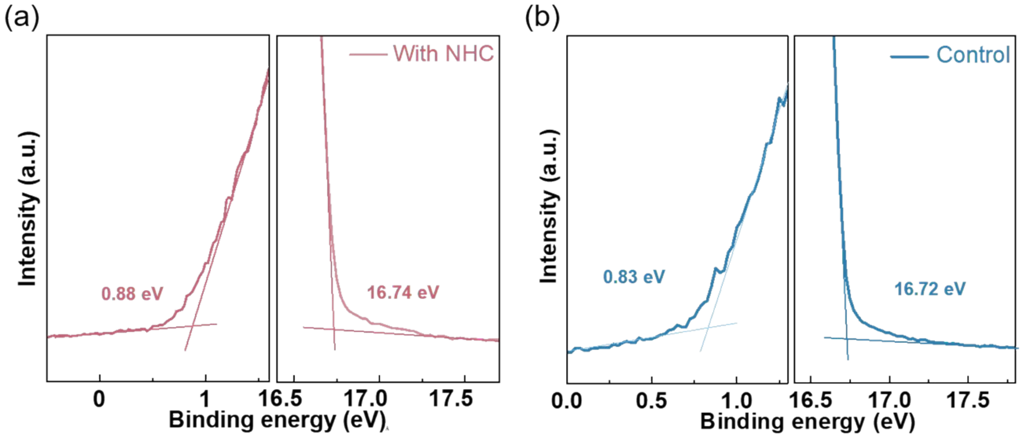

Figure S8. UPS data of the (a) control and (b) with NHC-treated perovskite films.

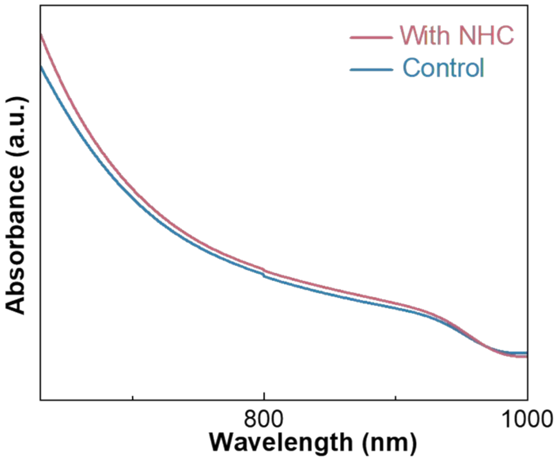

Figure S9. UV−vis absorption spectra of control and NHC-treated perovskite films.

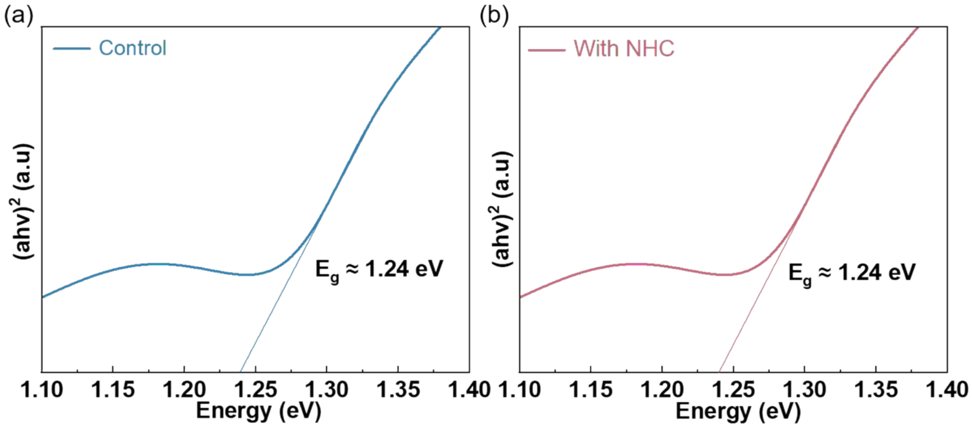

Figure S10. Tauc plots for (a) control and (b) with NHC-treated perovskite films.

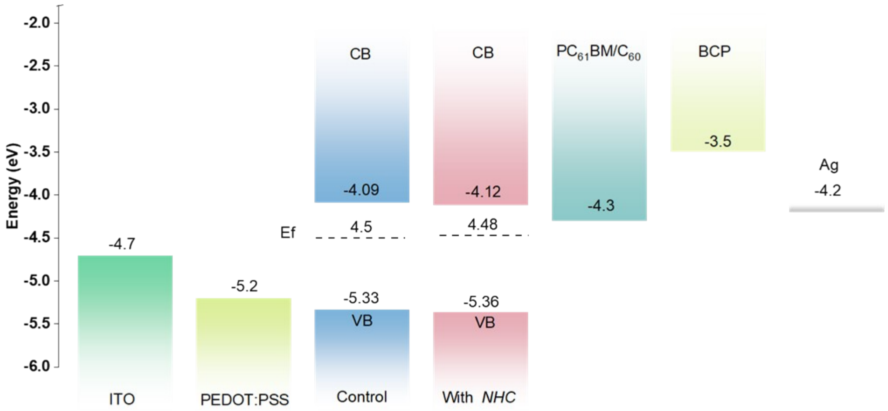

Figure S11. Energy level schemes derived from UPS spectra.

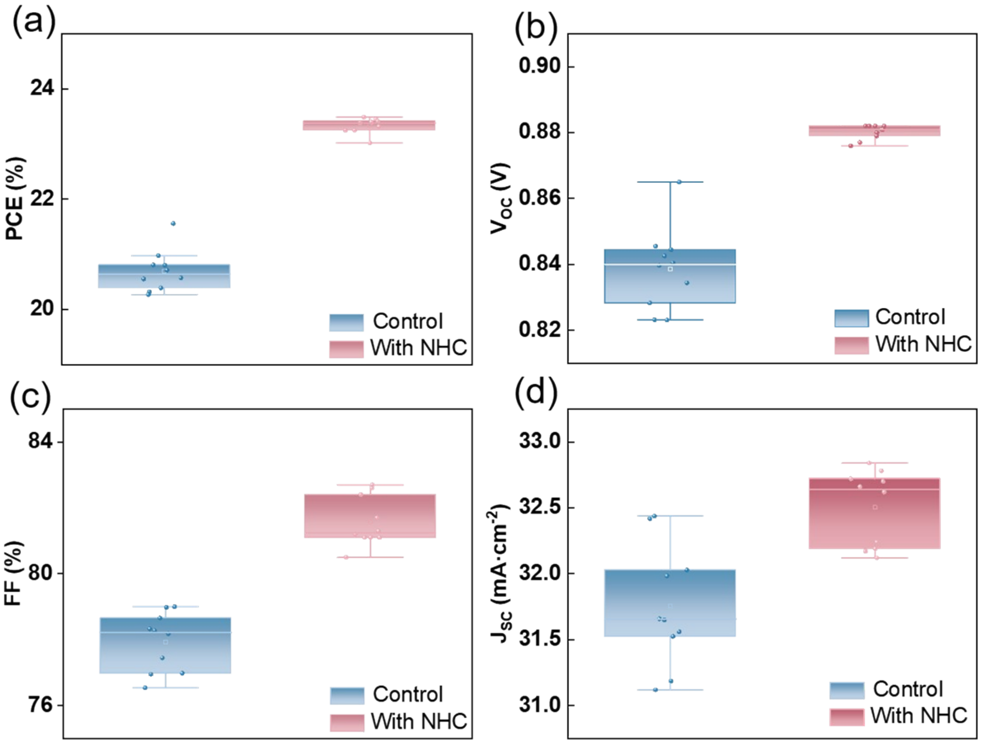

Figure R12. Performance parameters statistics of devices control and with NHC-treated devices: (a) PCE, (b) J_{SC}, (c) FF, and (d) V_{OC}.

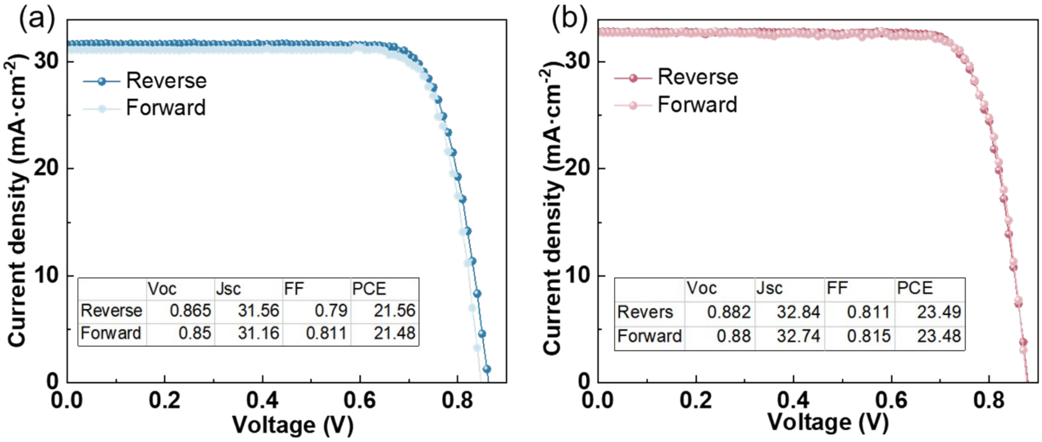

Figure S13. *J*–*V* curves of forward and reverse scanning directions for (a) control and (b) with NHC-treated devices.

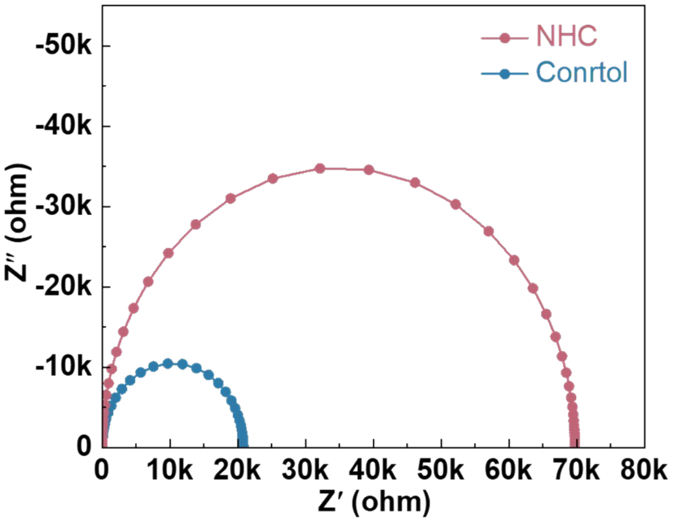

Figure S14. Nyquist plots of the devices with and without NHC treatment.

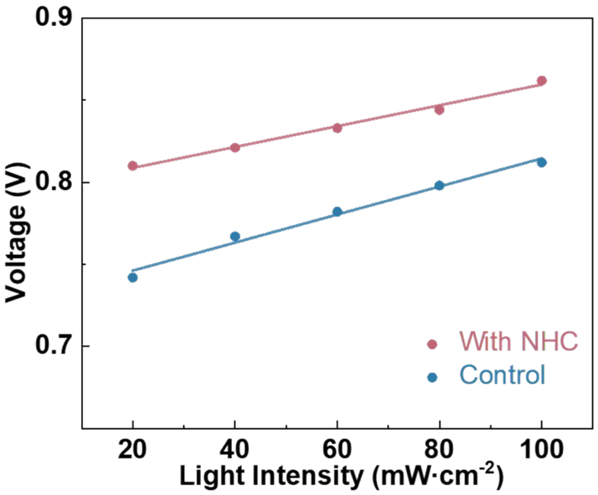

Figure S15. V_{OC} as a function of light intensity for control and NHC-treated perovskite devices.

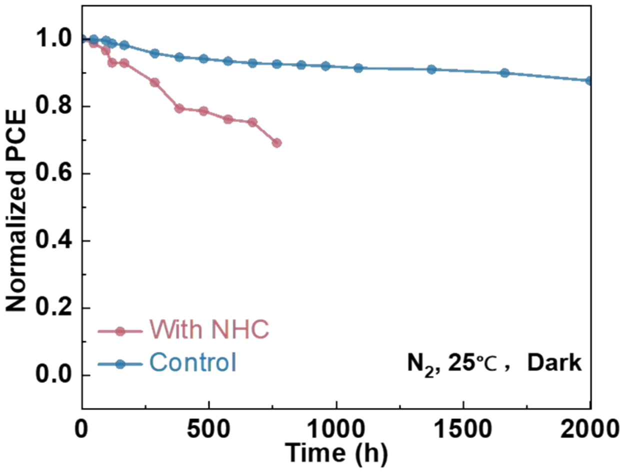

Figure S16. Storage stability of unencapsulated control and NHC-treated devices in N_2-filled glovebox.

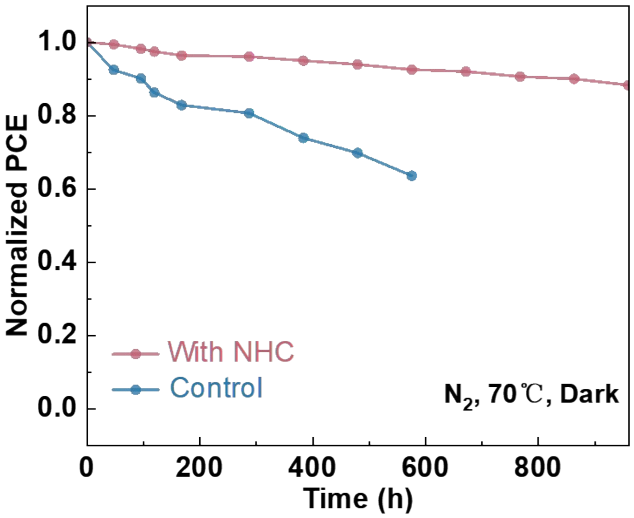

Figure S17. Thermal stability of unencapsulated control and NHC-treated devices.

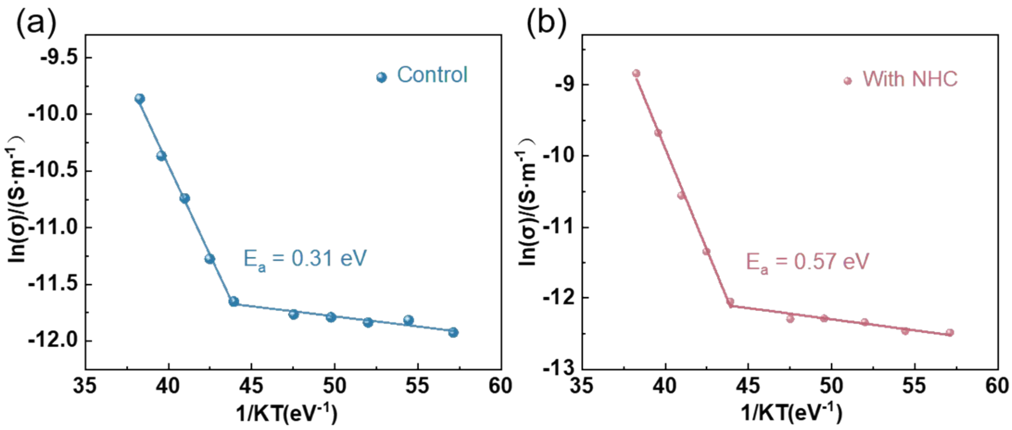

Figure S18. The temperature-dependent conductivity of the (a) control and (b) NHC-treated perovskite films.

Supplementary Table S1. FWHM of (100) and (200) diffraction planes for the control and NHC-treated perovskite films.

Perovskite film	FWHM (100)	FWHM (200)
Control	0.0842	0.1125
With NHC	0.0767	0.1095

Supplementary Table S2. Photovoltaic parameters of the devices with and without NHC treatment.

Sample	V_{OC} (V)	J_{SC} (mA·cm^{-2})	FF (%)	PCE (%)
Control	0.845	31.12	76.9	20.32
	0.842	31.65	78.6	20.97
	0.839	31.65	78.2	20.80
	0.834	32.02	76.9	20.57
	0.828	32.41	76.5	20.55
	0.840	31.52	78.1	20.71
	0.823	31.98	77.4	20.39
	0.823	32.43	78.3	20.27
	0.844	31.18	78.9	20.80
	0.865	31.56	79.0	21.56

Sample	V_{OC} (V)	J_{SC} (mA·cm^{-2})	FF (%)	PCE (%)
NHC	0.877	32.66	81.2	23.25
	0.876	32.72	80.5	23.25
	0.881	32.78	81.7	23.45
	0.882	32.62	81.1	23.32
	0.882	32.17	82.4	23.38
	0.882	32.19	81.1	23.02
	0.880	32.12	82.7	23.39
	0.879	32.24	82.6	23.4
	0.881	32.70	81.3	23.42
	0.882	32.84	81.1	23.49

(1) Wu, X.; Liu, Y.; Qi, F.; Lin, F.; Fu, H.; Jiang, K.; Wu, S.; Bi, L.; Wang, D.; Xu, F.; et al. Improved stability and efficiency of perovskite/organic tandem solar cells with an all-inorganic perovskite layer. *Journal of Materials Chemistry A* **2021**, *9* (35), 19778-19787, 10.1039/D0TA12286F. DOI: 10.1039/D0TA12286F.